

Effect of *Streptococcus mutans* on the Corrosion Behavior of Nano-Coating Ni-Cr Dental Alloy

M.A. Ameer^{1,*}, A.M. Fekry¹ and, May M.A. Bahr²

¹ Chemistry Department, Faculty of Science, Cairo University, Giza 12613, Egypt

² National Research Center, 33 El Bohouth St. P.O. 12311, Egypt

*E-mail: mameer_eg@yahoo.com,

Received: 19 May 2017 / Accepted: 28 July 2017 / Published: 12 September 2017

Corrosion behavior of chitosan, hydroxyapatite and TiO₂ nanoparticles (CS/TiO₂/HA) nano-layer Ni-Cr (Wiroloy) casting dental alloy and unlayered one were studied with time after exposing the tested alloys to fluoridated artificial saliva media without and/or with *streptococcus mutans* (*S.mutans*) Techniques used for corrosion examination were electrochemical impedance spectroscopy (EIS) and potentiodynamic techniques. SEM and EDX analysis was studied to characterize the layered film in absence or presence of bacteria. All measurements indicated that CS/TiO₂/HA nano-coating has high antibacterial effectiveness. Surface coverage increases with immersion time reaching a constant value after 72h and it was found to be 0.987 and 0.925 for CS/TiO₂/HA Nano-coating calculated from EIS and potentiodynamic techniques, respectively, after 6 days in presence of bacteria indicating the inactive property of the layer.

Keywords: *Streptococcus mutans* ; Chitosan; TiO₂; Hydroxyapatite; Wiroloy.

1. INTRODUCTION

A superior valuation of the deterioration route is linked among a full survey of the metal alloy biocompatibility [1-3]. Ni-Cr (Wiroloy) casting dental alloy was used in this study owing to its low cost and biocompatibility[2]. Modification of this dental alloy with surface layering materials may be useful for preventing the corrosion problems [1] especially due to *S. mutans* which is the main pathogen in the mouth causing dental caries. The chemical character of the metal alloy determines the elements of the apparent films that affects well on the corrosion behavior in simulated saliva [2]. Ni increases the strength, hardness, flexibility and ductility but it has allergic (female > male) gingival discoloration, swelling or redness effect, Cr increases tarnish and corrosion resistance by passive layer, Si and Mn increase the fluidity of the molten alloy and act as deoxidizer. Though the allergic nature of the metal ions of Ni-Cr based dental alloys should be well thought-out carefully, these alloys still

remain popular for dental use encouraging the interest of the current investigation. Low Cr and Mo causing a high dissolution speed and susceptibility to increase bacteria deposits[4]. An important parameter (also, an easy evaluation) for Ni-Cr-Mo-Fe alloys, is the relative effectiveness of Cr and Mo content on pitting or crevice corrosion usually that can be considered equivalent with pitting resistance equivalent (PRE) and can be calculated from [5]:

$$\text{PRE} = \% \text{Cr} + 3 \% \text{Mo} \quad (1)$$

A PRE value > 38 assumed to give good resistance to pitting corrosion in a Cl⁻ containing solution, as is the case of simulated saliva [5]. The Ni-Cr-Mo casting alloy is pitting resistant in simulated saliva when the PRE value increases up to approximately 49. For the investigated alloy, the PRE value for the pitting resistant of casting Wirloy is 26, which has moderate susceptible to pitting corrosion.

S. mutans (Gram-positive bacterium and a member of the human oral flora) is the primary cause in the formation of dental cavities in humans and is widely recognized for this [6]. A biofilm contains a well-ordered of microbial cells, including one or multi-species agglomerates, bounded by an extracellular matrix consisted of polysaccharides, nucleic acids, H₂O, proteins and other substances [7]. Biofilm precipitation is an fundamental part that can origin crashes of oral rehabilitation structures, particularly considering the pathogenic potential of some bacteria such as *S. mutans*, *Porphyromonas gingivalis* and *Prevotella* midway which encourage dental caries or periodontal diseases[8]. *S. mutans* is the utmost important due to its ability to liberate lactic acid and to develop in acidic environments becoming a powerful corrosive microorganism [7]. *S. mutans* is facultative anaerobic, gram-positive coccus (round bacterium) normally found in the human oral cavity and is a major contributor to tooth fragility [9].

The electrochemical study of the dental alloy in simulated saliva could be evaluated by using quick electrochemical technique as qualitative investigation to determine the corrosion resistance [10]. Corrosion on dental alloys could show biological, functional and aesthetic effects. If corrosion products are not biocompatible, the organism may be hurt due to the metal toxicity and the allergy threat. Therefore, the main object is dental alloy modification to minimize the metal ion release by developing a non-hazardous and successful treatment layer on alloy surface to improve dental alloy stability, bioperformance and resistance, which is essential for many applications [11].

In the present work, a new layer CS/HA/TiO₂ consists of chitosan, hydroxyapatite [HA, Ca₁₀(PO₄)₆(OH)₂] and TiO₂ nanoparticles[12] has been made to improve the corrosion resistance of Wirloy. The corrosion performance of non-layerd and/or nano-coatingrd (CS/HA/TiO₂) Wirloy, in absence and/or presence of *S. mutans*, were studied at 37°C with immersion time via electrochemical impedance spectroscopy (EIS) and potentiodynamic polarization techniques. The characterization of the surface is done by SEM and EDX techniques.

2. EXPERIMENTAL METHOD

2.1. Electrode preparation, cell and test solution

Wirloy was supplied by Bego (Bremen, Germany) and used as a working electrode; its

composition was: 63.5% Ni, 23 %Cr, 9 % Fe, 3% Mo, 1% Si, and 0.5 % Mn. Each specimen was in the form of a cylinder (area = 0.196 cm²). The mechanical properties and temperatures of casting dental alloys were: casting temperature (1340°C), Hardness HV (19), Elongation (355 N/mm²). A form of each alloy was formed by wax which had the requisite size in a ceramic cast. The cast was put in the Universal Burnout Furnace at high temperature (950–1000°C) for 2 h to dissolve and evaporate the wax, then the cast was filled with the molten alloy by centrifugal force using an induction casting machine. After that, specimens were polished with different grades (230-320-300-600-1200) of emery paper and then washed with distilled water. At the end, it dried with ethanol. All solutions were prepared using analytical grade chemicals.

2.2. Coating layer preparation

CS/TiO₂/HA Nano-coating was prepared by addition of chitosan to diluted acetic acid (1% w/w) and stirred for 5 hours to become transparent, and then the solution was filtered and stocked up at 4 °C. After that, TiO₂ and HA nanoparticles were added to chitosan solution and stirred for 5 hours and then it was used to coat the alloy surface and leaved to dry for 2 h before using and/or description[12]. The chemicals used in preparation of artificial saliva[13], with addition of 1000 ppm of NaF, are listed in Table 1.

Table 1. Composition of the stock fluoridated artificial saliva solution used in this work

Compound	ppm
NaCl	400
KCl	400
CaCl ₂ .2H ₂ O	795
Na ₂ S.9H ₂ O	5
NaH ₂ PO ₄ .2H ₂ O	690
Urea	1000
NaF	1000

2.3. Bacterial culture preparation

The samples were stored in desiccators for 1 day and sterilized before biofilm formation or electrochemical measurements by autoclaving at 121°C for 15 min. The artificial saliva was used as stock solution in vitro corrosion study. Bacterial strains and growth conditions *S.mutans* ATCC35668 were microaerophilically grown for 48 h at 37°C in agar plates with 32 g/L of BHI agar (Oxoid, England) supplemented with 3 g/L of yeast extract and 200 g/L of sucrose (Oxoid, England). The bacterial cells were inoculated in Tryptic Soy Broth (TSB, Bacto, Difco, USA) supplemented with 3 g/L of yeast extract and 200 g/L of sucrose for 18 h at 37°C and 150 rpm. After incubation, cells were harvested by centrifugation for 10 min at 48°C and 5000 rpm and washed twice with Phosphate Buffer Solution (PBS, Sigma–Aldrich, USA). Then, the cells were suspended in TSB supplemented with mucin (2.5 g/L), peptone (5 g/L), urea (1 g/L), yeast extract (2 g/L) and

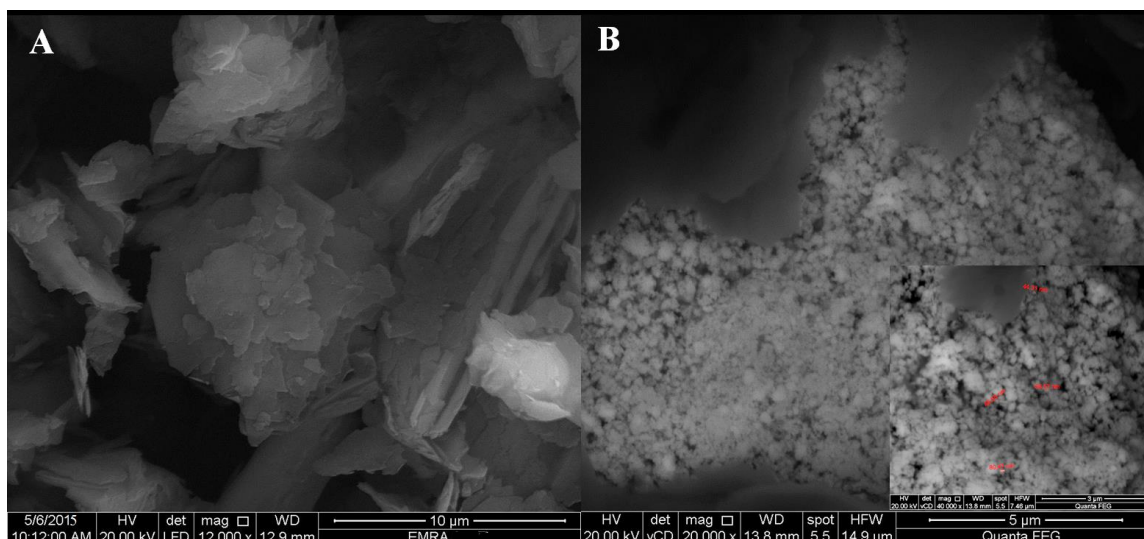
sucrose(200g/L)toobtainanopticaldensity(OD)ofabout0.6atA630,correspondingtoapproximately 1108CFU/ml⁴.The OD at 630 nm was measured using a spectrophotometer (Beckman Coulter,USA). This cell suspension was the inocula for biofilm formation assays. Biofilm formation and analysis Wirolloy samples were placed into24 well-plates, each containing 2ml of *S.mutans* inoculums (1108CFU/ml) and incubated at 37°C. After 24, 48, 72 and 144h (6days) of incubation, the samples were transferred for new well-plates and washed twice with PBS. The growth of bacterial colonies on the agar plates were taken out from the incubator and colony growth was appreciated. The time point was selected as a longer one in order to evaluate the increase of the concentration of bacterial culture spectrophotometrically and it's dependent on pH by using pH meter.

2.4. Instrumentation

For corrosion measurements, samples covered or not with *S.mutans* biofilms were mounted in an electrochemical cell connected to the external electrical system. The electrochemical techniques in this study were: impedance and potentiodynamic measurements. Impedance and polarization studies were conducted by connecting the electrochemical cell to the Auto EC-Lab® Software: Techniques and Applications Version 10.38–August2014. The frequency range was100 kHz–0.01Hz and the amplitude of the superimposed potential was 10 mV. All electrode potentials were measured with reference to the saturated calomel electrode, SCE, (Corning type). Surface study and morphology of casting surface sample of non-precious dental alloys were conducted by using a Scanning Electron Microscope SEM Model Quanta 250 FEG (Field Emission Gun) connected to EDX Unit (Energy Dispersive X-ray Analyses), with accelerating voltage 30 K.V., magnification14x up to 1000000 and resolution for Gun.1n) (FEI company, Netherlands).

3. RESULTS

3.1. Surfaces morphologies and films characterization in presence of *S.mutans*



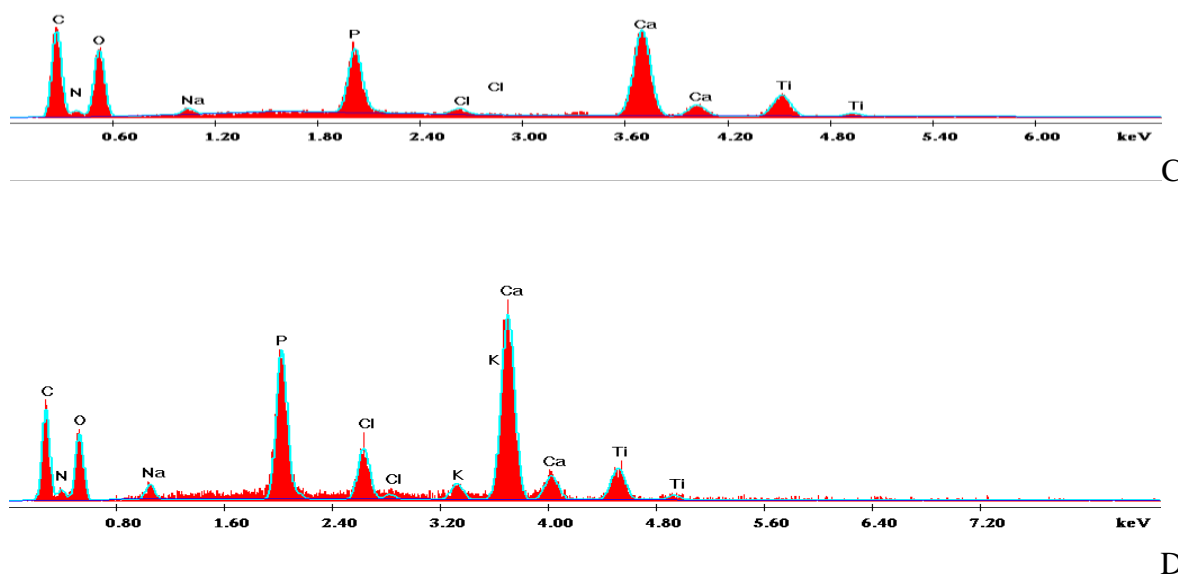


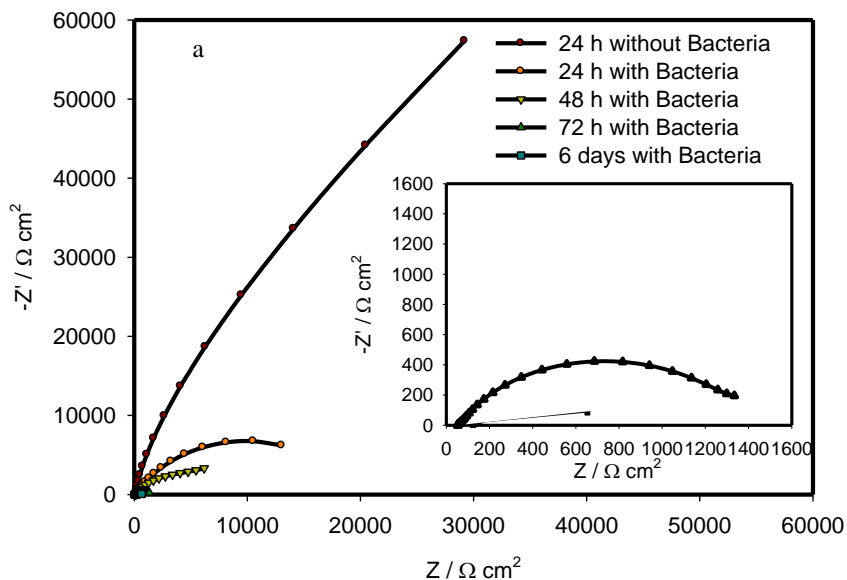
Figure 1. (a) SEM images for nanocoating Wirroloy after 6 days in absence of bacteria (b) SEM images for nanocoating Wirroloy after 6 days in in presence of bacteria. (c) EDX for nanocoating Wirroloy in absence of bacteria after 6 days (d) EDX for nanocoating Wirroloy in presence of bacteria after 6 days.

Figure 1 (a and b) shows the SEM images for CS/TiO₂/HA coating wirroloy in absence and in presence of bacteria, respectively. It is noticed that there is no difference between the two SEM images. This confirms that this layer has excellent antibacterial capability by its ability to attract bacteria [14].

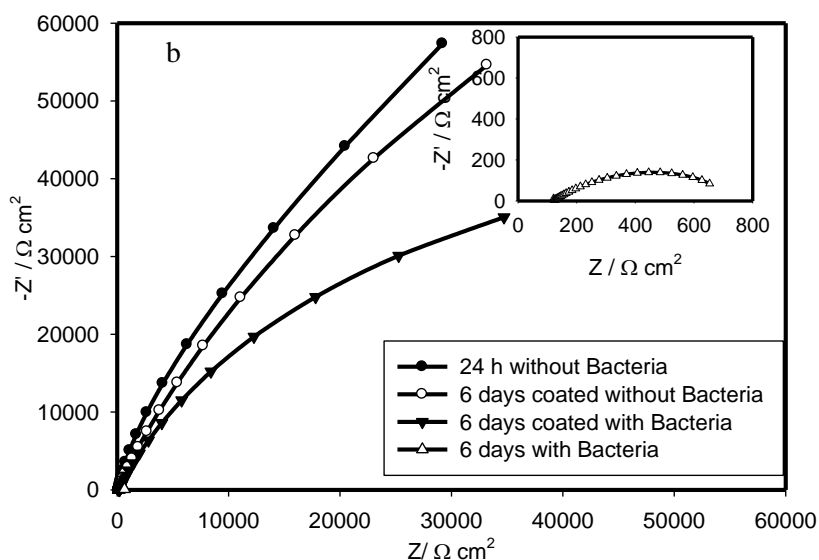
Fig.1(c & d) shows the EDX analysis for coating wirroloy in absence and in presence of bacteria, respectively. The elemental composition of EDX analyses (Fig.2c and d) for CS/TiO₂/HA Nano- layer confirms the presence of C, O, Ti and Ca, Cl elements that ensure the presence of HA, chitosan and TiO₂ in the layer. EDX investigation explains that almost the same Ti percentage (5.51, 5.83) or an increase of oxygen percentage (21.46, 31.24) on CS/TiO₂/HA nano-composite in absence and presence of bacteria, respectively, which may mean that the bacteria increases oxygen with a small percent leading to low corrosion in the presence of it. According to EDX analysis, it was noticed almost the same Ti percentage (5.51, 5.83) or an increase of oxygen percentage (21.46, 31.24) on CS/TiO₂/HA nano-composite in absence and presence of bacteria, respectively.

3.2. Impedance measurements

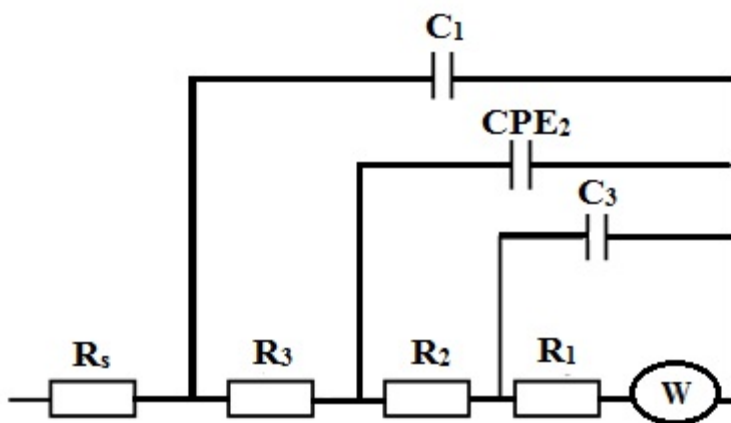
Impedance measurements can provide knowledge of the electrochemical performance of both the uncoating and Nano-coatingr coating electrodes. Figure 2 (a&b) shows Nyquist plots of Wirroloy electrode with different immersion time in artificial saliva at 37 °C. It is clear that the semicircle depresses highly with increasing time.



A



B



C

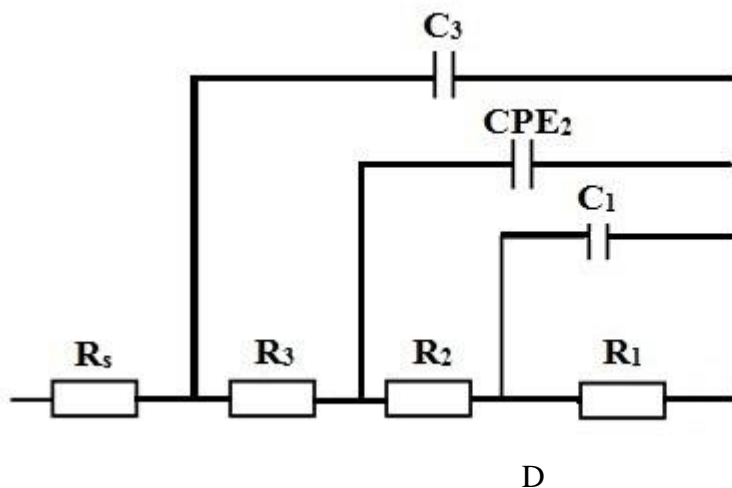


Figure 2. Impedance plots of Wiroloy in fluoridated artificial saliva with immersion time at 37 °C: (a) Nyquist plots for uncoating electrode. (b) Nyquist plots for coating electrode.(c)Three time constant equivalent circuit including Warburg impedance. (d)Three time constant equivalent circuit.

This means that the bacteria cause high corrosion. The best model that fits the experimental data is shown in Figure 2c & d. It is a three-time constant equivalent circuit model. This circuit considers three time constants: R_s =the solution resistance, C_1 and R_1 = impedance response to the diffusion, CPE_2 and R_2 = capacitance of the double layer and resistance to the charger transfer, C_3 and R_3 =capacitance and resistance due to the layering. W is the Warburg impedance due to the diffusion process. Three parallel capacitances are shown in the model: two of them are ideal (C_1 and C_3) and one is constant-phase element (CPE_2). A constant-phase element (CPE_2) was used instead of the ideal capacitance to account for surface heterogeneity [14].The impedance of CPE is $Z_{CPE} = [C(j\omega)^\alpha]^{-1}$, where $-1 \leq \alpha \leq 1$. The value of α is due to surface heterogeneity. The resistance and capacitance values for the non-coating and coating Wiroloy without and with bacteria are listed in Table 2. The best model that fits the other experimental data is shown in Figure 3b, which is the same for the previous model but without Warburg impedance indicating charge transfer process.

Table 2a. Impedance parameters for non-coating wiroloy in absence of bacteria at different immersion times in fluoridated artificial saliva, at 37°C. (Data are presented as the mean \pm S.D)

Time / hour	$R_3 / M\Omega cm^2$	$C_3 / \mu F cm^{-2}$	$R_2 / \Omega cm^2$	$CPE_2 / \mu F cm^{-2}$	α	$R_1 / \Omega cm^2$	$C_1 / \mu F cm^{-2}$	$W / k\Omega cm^2 s^{-1/2}$	$R_s / \Omega cm^2$
24	57.3 \pm 0.2	27 \pm 0.1	1670 \pm 0.2	12.4 \pm 0.2	0.60	200 \pm 0.3	5.4 \pm 0.2	-	117.8 \pm 0.1
48	55.4 \pm 0.1	29 \pm 0.2	1630 \pm 0.1	13.9 \pm 0.1	0.70	176 \pm 0.2	4.9 \pm 0.2	-	120.9 \pm 0.1
72	53.0 \pm 0.2	44 \pm 0.2	1567 \pm 0.1	17.2 \pm 0.1	0.59	165 \pm 0.2	4.0 \pm 0.1	-	122.9 \pm 0.1
144	50.3 \pm 0.1	54 \pm 0.3	1456 \pm 0.2	19.7 \pm 0.2	0.65	128 \pm 0.2	3.3 \pm 0.2	-	112.9 \pm 0.2

Table 2b. Impedance parameters for noncoating wirolloy in presence of bacteria at different immersion times in fluoridated artificial saliva, at 37°C. (Data are presented as the mean \pm S.D)

Time / hour	$R_3 / \text{M}\Omega \text{ cm}^2$	$C_3 / \mu\text{F cm}^{-2}$	$R_2 / \Omega \text{ cm}^2$	$\text{CPE}_2 / \mu\text{F cm}^{-2}$	α	$R_1 / \Omega \text{ cm}^2$	$C_1 / \mu\text{F cm}^{-2}$	$W / \text{k}\Omega \text{ cm}^2 \text{ s}^{-1/2}$	$R_s / \Omega \text{ cm}^2$
24	20.98 \pm 0.2	51 \pm 0.2	1400 \pm 0.2	25.8 \pm 0.2	0.70	171 \pm 0.2	6.7 \pm 0.2	3.1 \pm 0.2	134.4 \pm 0.1
48	9.6 \pm 0.2	66 \pm 0.2	995 \pm 0.2	54.5 \pm 0.2	0.72	154 \pm 0.2	6.9 \pm 0.2	3.1 \pm 0.2	113.8 \pm 0.2
72	1.5 \pm 0.2	75 \pm 0.3	830 \pm 0.2	57.6 \pm 0.1	0.69	129 \pm 0.2	7.3 \pm 0.2	8.8 \pm 0.2	90.28 \pm 0.2
144	0.6 \pm 0.2	83 \pm 0.2	605 \pm 0.3	71.8 \pm 0.2	0.61	96.9 \pm 0.2	7.4 \pm 0.2	20.9 \pm 0.2	64.7 \pm 0.2

Table 2C. Impedance parameters for nanocoating wirolloy in absence of bacteria at different immersion time in fluoridated artificial saliva at 37°C. (Data are presented as the mean \pm S.D)

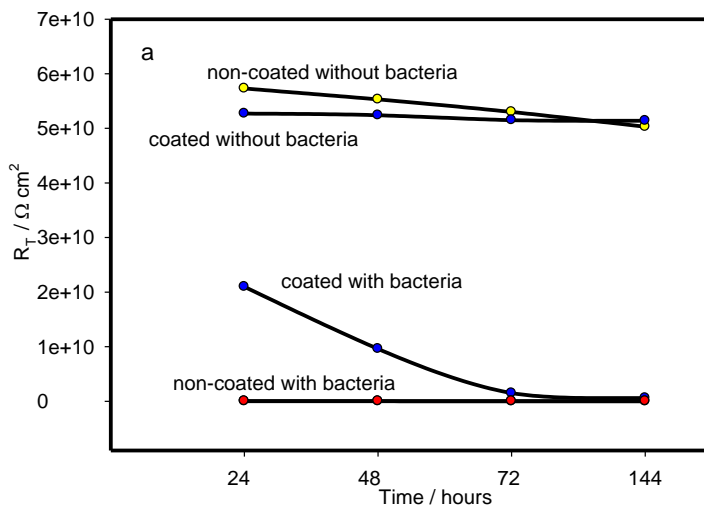
Time / hour	$R_3 / \text{M}\Omega \text{ cm}^2$	$C_3 / \mu\text{F cm}^{-2}$	$R_2 / \Omega \text{ cm}^2$	$\text{CPE}_2 / \mu\text{F cm}^{-2}$	α	$R_1 / \Omega \text{ cm}^2$	$C_1 / \mu\text{F cm}^{-2}$	$W / \text{k}\Omega \text{ cm}^2 \text{ s}^{-1/2}$	$R_s / \Omega \text{ cm}^2$
24	52.7 \pm 0.2	20.5 \pm 0.2	1800 \pm 0.2	25.8 \pm 0.2	0.60	400 \pm 0.2	6.7 \pm 0.2	-	134.4 \pm 0.1
48	52.4 \pm 0.2	31.2 \pm 0.1	1695 \pm 0.2	54.5 \pm 0.2	0.70	294 \pm 0.2	6.9 \pm 0.3	-	113.8 \pm 0.2
72	51.7 \pm 0.2	33.1 \pm 0.2	1600 \pm 0.2	57.6 \pm 0.3	0.55	229 \pm 0.2	7.3 \pm 0.3	-	90.28 \pm 0.1
144	51.4 \pm 0.3	35 \pm 0.2	1590 \pm 0.2	15.1 \pm 0.2	0.65	193 \pm 0.2	5.8 \pm 0.2	-	120.8 \pm 0.1

Table 2d. Impedance parameters for nanocoating wirolloy in presence of bacteria at different immersion time in fluoridated artificial saliva at 37°C. (Data are presented as the mean \pm S.D.)

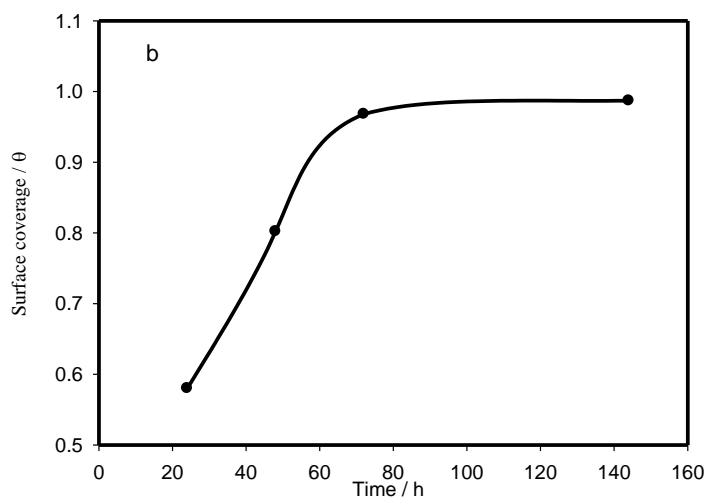
Time / hour	$R_3 / \text{M}\Omega \text{ cm}^2$	$C_3 / \mu\text{F cm}^{-2}$	$R_2 / \Omega \text{ cm}^2$	$\text{CPE}_2 / \mu\text{F cm}^{-2}$	α	$R_1 / \Omega \text{ cm}^2$	$C_1 / \mu\text{F cm}^{-2}$	$W / \text{k}\Omega \text{ cm}^2 \text{ s}^{-1/2}$	$R_s / \Omega \text{ cm}^2$
24	49.98 \pm 0.2	28 \pm 0.2	2400 \pm 0.2	15.8 \pm 0.2	0.66	221 \pm 0.2	5.7 \pm 0.2	-	60.1 \pm 0.2
48	48.6 \pm 0.2	29 \pm 0.2	1995 \pm 0.2	14.5 \pm 0.2	0.70	214 \pm 0.2	5.9 \pm 0.2	-	55.9 \pm 0.2
72	47.5 \pm 0.2	35 \pm 0.2	1830 \pm 0.2	17.6 \pm 0.2	0.69	200 \pm 0.2	6.3 \pm 0.2	-	70.28 \pm 0.2
144	47.1 \pm 0.2	39 \pm 0.2	1431 \pm 0.2	17.3 \pm 0.2	0.60	187 \pm 0.2	6.1 \pm 0.2	-	53.8 \pm 0.2

The total resistance, R_T , values for nanocoating alloy in presence of bacteria decrease with increasing time, with lower values (39.8 $\text{M}\Omega \text{ cm}^2$) than those of nanocoating alloy in absence of bacteria (51.4 $\text{M}\Omega \text{ cm}^2$) after 6 days of immersion in artificial saliva (Table 2a). The same model in Fig. 4a is used to fit its data. It is clear that Warburg impedance appeared at 24, 48, 72 and 144h for

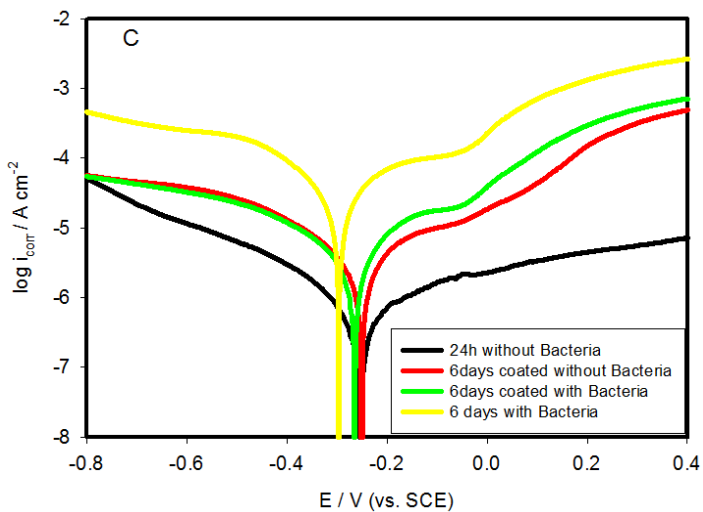
non-coating alloy in presence of bacteria. This proves that the corrosion reactions at these cases are under diffusion phenomena. Fitting data is given in Table 2b.



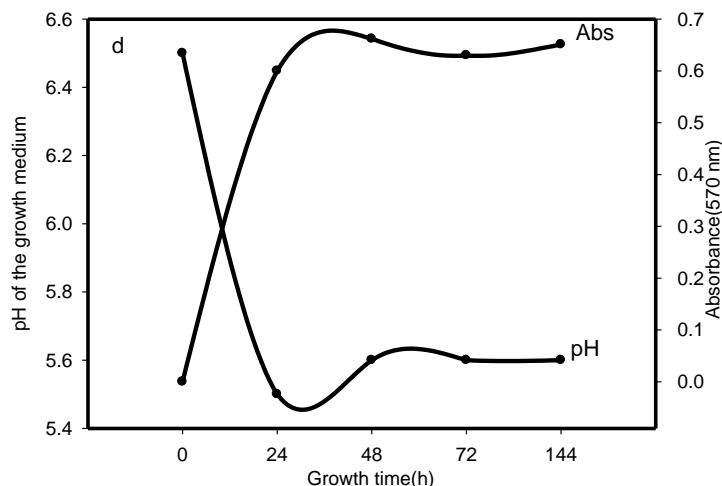
A



B



C



D

Figure 3. (a) Variation of Total resistance (R_T) with time for the uncoating and coating alloy in absence and presence of bacteria in fluoridated artificial saliva at 37 °C.(b)Variation of surface coverage with time for coating alloy in presence of bacteria in fluoridated artificial saliva at 37 °C.(c) Polarization scans for alloy after immersion for 24h and 6 days in fluoridated artificial saliva at 37 °C.(d) Absorbance (Abs) of *S. mutans* biofilm formed on alloy surfaces and pH of biofilm medium after 24, 48, 72 and 144 h (6 days) of growth.

From the proposed model, it is clear that the inactive film includes three layers and the protection efficiency is mostly due to the outer layer. CS/TiO₂/HA nano-coating gives a higher outer barrier resistance (R_3) value of 39MΩ cm² compared to 0.6 MΩ cm² for the non-coating alloy in presence of bacteria.

Fig. 3a illustrates the relation between the total resistance (R_T) and time for the alloy in fluoridated artificial saliva at 37 °C with its schematic.

The surface coverage (θ) for the nano-coating was calculated using the next equation [15]:

$$\theta = \frac{R_T - R_T^\circ}{R_T} \tag{2}$$

where R_T° and R_T are the total resistances for both the unlayerd and nano-coatingrd alloy, respectively in presence of bacteria. The results are given in Fig.3b; it is found that the surface coverage increases with immersion time and reaching constant value after 72h.

3.3. Potentiodynamic polarization measurements

Potentiodynamic polarization technique was done to obtain knowledge about the corrosion characterization of the formed layers, where the corrosion rate is proportional to the corrosion current density. Potentiodynamic polarization measurements were done in the range from -1.5 V to 2.0V vs. SCE (Fig.6), at a scan rate of 1.0 mVs⁻¹ in fluoridated artificial saliva after reaching steady state potential value, at 37°C. Polarization parameters (i_{corr} , E_{corr} , β_a and β_c) were given in Table 3.The

corrosion potential (E_{corr}) and corrosion current density (i_{corr}), equivalent to corrosion rate, is given by the intersection of the Tafel lines extrapolation [16]. Anodic and cathodic Tafel constants are symbolized, respectively as follows, β_a and β_c . They are estimated from the anodic and cathodic slopes of Tafel plot [16].

Table 3. Corrosion parameters of non-layerd and nanocoating wiroloy in absence and presence of bacteria in fluoridated artificial saliva at different immersion at 37°C. (Data are presented as the mean \pm S.D.)

Time H	β_a mV/dec	$-\beta_c$ mV/dec	i_{corr} $\mu\text{A cm}^{-2}$	E_{corr} mV
24h without Bacteria	224 \pm 0.2	157 \pm 0.2	1.09 \pm 0.2	-253 \pm 0.2
24h with Bacteria	187 \pm 0.2	174 \pm 0.2	13.5 \pm 0.2	-293 \pm 0.2
24h layerd without Bacteria	188 \pm 0.3	176 \pm 0.3	1.5 \pm 0.3	-245 \pm 0.3
24h layerd with Bacteria	189 \pm 0.3	171 \pm 0.3	3.5 \pm 0.3	-255 \pm 0.3
48 h with Bacteria	193 \pm 0.2	169 \pm 0.2	19.9 \pm 0.2	-293 \pm 0.2
72 h with Bacteria	197 \pm 0.2	171 \pm 0.2	28 \pm 0.2	-296 \pm 0.2
6 days with Bacteria	203 \pm 0.2	160 \pm 0.2	67 \pm 0.2	-306 \pm 0.2
6 days layerd with Bacteria	205 \pm 0.2	167 \pm 0.2	5.0 \pm 0.2	-275 \pm 0.2
6 days layerd without Bacteria	212 \pm 0.2	170 \pm 0.2	3.6 \pm 0.2	-259 \pm 0.2

The E_{corr} value for the tested non coating alloy revealed that it was shifted towards more negative values as the time increases in presence of bacteria. After 6 days, E_{corr} value shifted to more positive value in the following order: non coating with bacteria (-306 mV) nano coating with bacteria - 275 mV < nano coating without bacteria (-259 mV). Also i_{corr} values decreased in the same order, indicating that CS/TiO₂/HA nano-coating without bacteria has the lowest i_{corr} value (3.6 $\mu\text{A cm}^{-2}$) and the non-layerd alloy in presence of bacteria has the highest i_{corr} value (67 $\mu\text{A cm}^{-2}$) with the highest corrosion rate. However, adding CS/TiO₂/HA nano-coating decrease the corrosion rate because chitosane is a macromolecule adsorbed well on the surface through electron pairs [17].

The surface coverage (θ) for the nanolayer after 6 days was calculated using the following equation [15]:

$$\theta = \left[1 - \frac{i_{\text{coating}}}{i_{\text{uncoating}}} \right] \quad (3)$$

Where $i_{\text{uncoating}}$ and i_{coating} are the corrosion current densities for uncoating and nanocoating alloy in presence of bacteria, respectively (after 6 days). It was found that θ for CS/TiO₂/HA is reaching to 0.925.

Figure 3c, illustrates the absorbance (Abs) of *S. mutans* culture medium and pH of biofilm medium after 24, 48, 72 and 144 h (6 days) of growth. It is clear that the biomass of *S. mutans* biofilms formed on samples was determined after 24, 48, 72, and 144 h by absorbance measurements of culture medium (Fig.3c). A significant increase in concentration (absorbance) occurs after 24 h of incubation. However, no statistically significant differences were found between the biomass present after 24 and 144 h (6 days) of incubation. Also, as shown in Fig. 3c, the pH of the growth medium becomes acidic during the growth of the biofilm.

4. DISCUSSION

SEM images confirm that the CS/TiO₂/HA nano layer has excellent antibacterial efficiency by its ability to absorb bacteria¹⁸. According to EDX analysis, there is almost the same Ti percentage or an increase of oxygen percentage on CS/TiO₂/HA nano-layer in absence and presence of bacteria, constancy with high adsorption properties to the alloy surface giving highest surface coverage for the tested alloy by giving vastly dense surface layer.

In general, TiO₂ may be adsorbed on HA in chitosan through positively charged calcium ions in HA forming calcium titanate CaTiO₃ as follows [12-14, 19]:



It is noticed that adding TiO₂ in chitosan matrix decreased well the corrosion rate by increasing the film strength and then adding HA gives the lowest corrosion rate. This is due to the adsorption of both TiO₂ and HA nanoparticles to the alloy surface which is simulated by the presence of CS. So, CS/HA/TiO₂ nanostructure impenetrable layering acts well as a hindrance to the transfer of electrons and ions between the alloy and the artificial saliva. So, this nano-coating improved well the corrosion resistance of the alloy surface.

The surface coverage, θ , which obtained by impedance measurements is near to that obtained from polarization measurements. Thus, polarization results confirm well impedance measurements. This is confirmed well by its high corrosion resistance calculated from all used electrochemical and surface techniques.

In fact, oral biofilms with a large quantity of *S.mutans* make a decline in pH of the oral cavity which promoting the dentine as well as the corrosion of dental curative materials. However, the corrosive function of *S.mutans* depends on the sucrose concentration present on its environment and in its bond to the oral surfaces [16, 17]. While *S.mutans* is not the only cause directly for periodontal inflammations, it is known that oral biofilms consist in consortia of other species depending on environmental circumstances like oxygen, nutrients, and pH[17]. In addition, the biofilm composition can pick up external acidic substances from nutritional and that produced from microbial metabolism [20].

5. CONCLUSIONS

The electrochemical behavior of cast Wiroloy in absence and presence of *S.mutans* and non-toxic nanolayer was studied. The subsequent conclusions were investigated:

1. SEM and EDX analysis of the films in absence and presence of bacteria after 6 days indicated that CS/TiO₂/HA nano-layer has antibacterial effectiveness.
2. An electric equivalent circuit with three time constants model was used for layered and unlayered alloy.
3. CS/TiO₂/HA nano-coating has excellent corrosion resistance because it has almost complete coverage of alloy surface protecting it from corrosion.

4. Higher R_T ($47 \text{ M}\Omega \text{ cm}^2$) and lowest corrosion current density ($5.0 \mu\text{A cm}^{-2}$) was observed for CS/TiO₂/HA nano-coating with surface coverage reaching to 0.987 after 6 days due to the enhancement of the protective properties of the inactive property for this layer.

So, CS/TiO₂/HA nano-coating is an important layer to be useful for dentistry.

References

1. A. Fahmy, A. Hamed, M. Gobashy, *Journal of American Sci.*, 8 (2012) 804.
2. M. Ameer, E. Khamis, M. Al-Motlaq, *Corr. Sci.*, 46 (2004) 2825.
3. H.A. Ching, D. Choudhury, M.J. Nine, N.A.A. Osman, *Sci Technol Adv Mater.*, 15(2014) 1.
4. E. Gatin, D. Pirvu, R. Cara, *Dig. J. Nanomater. Bios.*, 6 (2011) 1333.
5. J.K. Clarke, *Br J Exp Pathol.*, 5 (1924) 141.
6. P.D. Marsh, M.V. Martin, M.A. Lewis, D. Williams, *Oral Microbiology*, Elsevier Health Sciences, 2009.
7. D.H. Limoli, C.J. Jones, D.J. Wozniak, *Microbiol Spectr.*, 3 (2015) 1.
8. K. J. Ryan, W. L. Drew, J. J. Plorde, N. Ahmad, K. Ryan, *Hardcover, Published by Mcgraw-Hill Europe International Edition*, 2010.
9. G.M. El Sherbiny, *Int. J. Curr. Microbiol. App. Sci.*, 3 (2014) 1.
10. D. Mareci, G. Nemtoi, N. Aelenei, C. Bocanu, *Eur Cell Mater.*, 10 (2005) 1.
11. S. Arango, A. Peláez-Vargas, C. García, *Layerings*. 3 (2013) 1.
12. A.M. Fekry, *RSC Adv.*, 6 (2016) 20276.
13. T. Fusayama, T. Katayori, S. Nomoto, *J Dent. Res.*, 42(1963) 1183.
14. M. Ameer, A. Fekry, *Int J Hydrogen Energy*, 35 (2010) 11387.
15. A. Fekry, A. Ghoneim, M. Ameer, *Surf. Coat. Technol.*, 238 (2014) 126.
16. A. Corbin, B. Pitts, A. Parker, P.S. Stewart, *Antiviral Chem. Chemother.*, 55 (2011) 3338.
17. J.C. Souza, P. Ponthiaux, M. Henriques, R. Oliveira, W. Teughels, J.-P. Celis, L.A. Rocha, *J Dent.*, 41 (2013) 528.
18. M. Dash, F. Chiellini, R. Ottenbrite, E. Chiellini, *Prog. Org. Layer*, 36 (2011) 981.
19. A. Ghoneim, A. Fekry, M. Ameer, *Electrochim. Acta*, 55 (2010) 6028.
20. Y. Li, R.A. Burne, *Microbiol.*, 47 (2001) 2841.